

# Probe Higgs-gluon coupling via jet energy profile at $e^+e^-$ colliders

Gexing Li,<sup>1,2,\*</sup> Zhao Li,<sup>1,2,†</sup> Yandong Liu,<sup>3,4,‡</sup> Yan Wang,<sup>1,5,§</sup> and Xiaoran Zhao<sup>6,¶</sup>

<sup>1</sup>*Institute of High Energy Physics, Chinese Academy of Sciences, Beijing 100049, China*

<sup>2</sup>*School of Physics Sciences, University of Chinese Academy of Sciences, Beijing 100039, China*

<sup>3</sup>*Key Laboratory of Beam Technology of Ministry of Education,*

*College of Nuclear Science and Technology, Beijing Normal University, Beijing 100875, China*

<sup>4</sup>*Beijing Radiation Center, Beijing 100875, China*

<sup>5</sup>*Deutsches Elektronen-Synchrotron, Hamburg 22607, Germany*

<sup>6</sup>*Centre for Cosmology, Particle Physics and Phenomenology (CP3),  
Université catholique de Louvain, 1348 Louvain-la-Neuve, Belgium*

The effective coupling of Higgs boson to gluon pair is one of the most important parameters to test the Standard Model and search for the new physics beyond. In this paper, we propose several new observables based on jet energy profile to extract the effective coupling. The statistical uncertainties of the effective coupling extracted by using new observables are derived and estimated based on the simulation at the future  $e^+e^-$  collider for 250 GeV center-of-mass energy and  $5 \text{ ab}^{-1}$  integrated luminosity. We found the statistical uncertainties of effective coupling via the optimized observable can reach about 1.6% in the channels of  $Z$  boson decaying to lepton pairs and is reduced by 52% compared to the relevant uncertainties in conventional approach. These new observables potentially can be helpful for the measurement of effective coupling at the future  $e^+e^-$  colliders.

PACS numbers: 13.66.Fg, 14.70.Dj, 14.80.Bn

## INTRODUCTION

The discovery of Higgs boson at the CERN Large Hadron Collider (LHC) has marked the completeness and success of the Standard Model (SM). Thereafter the precision measurement on the properties of Higgs boson has become the most promising approach to completely understanding the Higgs mechanism, since the SM predicts not only one scalar boson but also the couplings of Higgs boson to the other SM particles. The effective coupling of Higgs boson to gluon pair is one of the most important parameters to test the Standard Model and thus to search for the new physics beyond, since it can be directly affected by the new physics particle loop [1–8]. However, due to the limited accuracy at the LHC, most of the properties of Higgs boson cannot be thoroughly investigated [9, 10]. Therefore, the next generation of electron-positron collider becomes an inevitable choice due to its clean environment.

In the past few years, several options have been proposed as Higgs factory, for instance, Circular Electron-Positron Collider (CEPC) [11–13], Future Circular Collider-electron-positron (FCC-ee) [14–16] and International Linear Collider (ILC) [17–19]. At the Higgs factory, the measurement on most of the Higgs properties can be expected to reach a high accuracy. And ideally the Higgs-gluon coupling can be investigated by extracting the  $gg$  mode in Higgs boson decays. With b-tagging efficiency 80%, the accuracy of Higgs-gluon coupling will reach to 2.2% for the channels of  $Z$  boson decaying to lepton pair before using template fit, and can be further improved to 1.5% after using template fit[20].

However, according to the SM predictions on the decays of 125 GeV Higgs boson [21, 22], the  $gg$  mode has

very small branching ratio  $\mathcal{B}_{gg}^{\text{SM}} \equiv \mathcal{B}^{\text{SM}}(h \rightarrow gg) = 8.56\%$  and phenomenologically manifests di-jet signals. Meanwhile the  $b\bar{b}$  mode ( $\mathcal{B}_{b\bar{b}}^{\text{SM}} \equiv \mathcal{B}^{\text{SM}}(h \rightarrow b\bar{b}) = 58.09\%$ ) and  $c\bar{c}$  mode ( $\mathcal{B}_{c\bar{c}}^{\text{SM}} \equiv \mathcal{B}^{\text{SM}}(h \rightarrow c\bar{c}) = 2.9\%$ ) have sizable contributions to the di-jet events. This would seriously drawback the efficiency to extract the Higgs-gluon coupling.

In the view of experiment observation, the di-jet decay mode of Higgs boson has dominant contribution from bottom quark pair so the Higgs-gluon coupling is overwhelmed. To reveal Higgs-gluon coupling from Higgs decay, b-tagging is an efficient tool to suppress bottom quark contribution. However, the b-tagging is not enough to fully eliminate the quark-jets from Higgs boson decay and the background processes to Higgs production. Therefore, it is worthy to elaborate other approaches to promote the branching ratio measurement.

One longstanding and extensively studied goal at the collider is how to efficiently distinguish the jets induced by quark and gluon. Of all the proposed variables to achieve the goal, jet energy profile (JEP) is conventional one. For a jet of cone size  $R$ , the JEP is defined as

$$\psi(r) = \frac{1}{N_j} \sum_j \psi_j(r) = \frac{1}{N_j} \sum_j \frac{\sum_{r_i < r} p_{T,i}(r_i)}{\sum_{r_i < R} p_{T,i}(r_i)}, \quad (1)$$

where  $r$  ( $\leq R$ ) is the size of a test cone.  $N_j$  is the total number of jets.  $p_{T,i}$  and  $r_i$  are the transverse momentum and the distance from jet axis of the  $i$ -th constituent, respectively. And  $\psi_j(r)$  represents the JEP of a single jet, so  $\psi(r)$  can also be defined as the average JEP of jets. Generally gluon jet has different JEP shape from quark-jet due to more QCD radiations. Since the

usually observed jets are the mixing of quark-jets and gluon-jets, the overall JEP would be the weighted average of quark-jet JEP and gluon-jet JEP and its shape can imply the ratio between quark-jets and gluon-jets. Many works have utilized the JEP to improve the analysis, for instance, identifying Higgs production mechanisms [23], searching for dark matter interactions [24], and detecting new physics in di-jet resonance [25].

In this paper, we assume the new physics influences only the Higgs-gluon coupling and can be summarized into the effective operator of Higgs-gluon-gluon interaction[3]

$$\mathcal{L}_{hgg} = \kappa_g c_{\text{SM}}^g \frac{\alpha_s}{12\pi v} h G_{\mu\nu}^a G^{a\mu\nu}, \quad (2)$$

where  $c_{\text{SM}}^g$  is the SM prediction of Higgs-gluon effective coupling from heavy quark loop.  $\kappa_g$  represents the deviation from the SM prediction, i.e.  $\kappa_g = 1$  in the SM. By analyzing the di-jet decay mode of Higgs boson that is produced via the process  $e^+e^- \rightarrow Zh$  at the future  $e^+e^-$  collider, instead of conventional averaged JEP shown in Eq.(1) we extract the information of  $\kappa_g$  from the accumulated JEP, which has better sensitivity to  $\kappa_g$  and will be explained in detail in the next section. In the analysis the b-tagging and c-tagging are included to suppress the contribution from bottom pair and charm pair decay modes.

The content is organized as follows. In the next section, several observables are defined based on JEP, and the relevant uncertainties of  $\kappa_g$  via different observables are derived. In the third section, the Monte-Carlo (MC) simulation including background events is used for comparison between different observables at future  $e^+e^-$  collider. Then conclusion is made in the final section.

## ACCUMULATED JET ENERGY PROFILE

Suppose the new physics beyond the SM could modify the Higgs-gluon effective operator as shown in Eq.(2), the partial width of Higgs decay to gluon pair will change accordingly and the total width of Higgs boson will also be changed. Consequently all the decay branching ratios of Higgs boson will not be the same as predicted by the SM. However, according to the measurement on the Higgs production total cross section via gluon fusion at the LHC [26, 27], the deviation of  $\kappa_g$  from the SM cannot be larger than 10%. Also since the branching ratio of Higgs decay to gluon pair is only 8.56%, the effect of  $\kappa_g$  variation on the other decay branching ratios would be less than 0.1%, which is already smaller than the expected experiment errors at the Higgs factory. Therefore, in this work we assume the new physics effect only affects the decay branching ratio  $\mathcal{B}_{gg} \approx \kappa_g^2 \mathcal{B}_{gg}^{\text{SM}}$  while the other branching ratios are approximately unchanged, e.g.  $\mathcal{B}_{bb} \approx \mathcal{B}_{bb}^{\text{SM}}$ . Therefore, by the definition in Eq.(1) the energy profile of jets from the Higgs di-jet decay channel

can be explicitly expressed as

$$\psi(r) = \frac{\kappa_g^2 \mathcal{B}_{gg}^{\text{SM}} \psi_g + \mathcal{B}_{q\bar{q}}^{\text{SM}} \psi_q}{\kappa_g^2 \mathcal{B}_{gg}^{\text{SM}} + \mathcal{B}_{q\bar{q}}^{\text{SM}}}, \quad (3)$$

where  $\psi_g$  and  $\psi_q$  are the energy profiles of gluon-jet and quark-jet, respectively. And

$$\mathcal{B}_{q\bar{q}}^{\text{SM}} \equiv \mathcal{B}_{bb}^{\text{SM}}(1 - \varepsilon_b)^2 + \mathcal{B}_{c\bar{c}}^{\text{SM}}(1 - \varepsilon_c)^2. \quad (4)$$

Here the quark-jet is composed of charm-jet and bottom-jet, and the JEP of quark-jet is obtained by the weighted average of JEP of charm-jet and bottom-jet. Meanwhile, in order to increase the sensitivity of JEP to  $\kappa_g$  both the b-tagging and c-tagging (b&c-tagging) have been applied to suppress the contributions from bottom-jet and charm-jet. And  $\varepsilon_b$  and  $\varepsilon_c$  are the efficiencies of b-tagging and c-tagging, respectively.

In the above equation, the decay branching ratios  $\mathcal{B}_{gg}^{\text{SM}}$ ,  $\mathcal{B}_{bb}^{\text{SM}}$  and  $\mathcal{B}_{c\bar{c}}^{\text{SM}}$  can be obtained by the SM predictions, and the JEP of quark-jet and gluon-jet,  $\psi_q$  and  $\psi_g$ , can be obtained by MC simulation or perturbative QCD prediction[28].

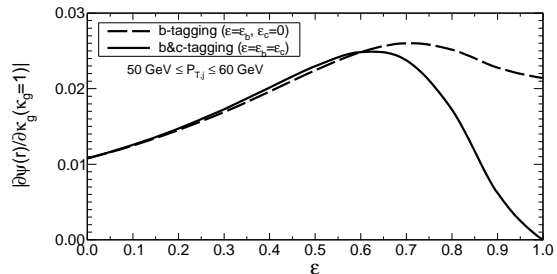


FIG. 1: The slopes of JEP with respect to  $\kappa_g$  at  $\kappa_g = 1$  as function of tagging efficiency  $\varepsilon$  after b-tagging( $\varepsilon = \varepsilon_b, \varepsilon_c = 0$ ) and b&c-tagging( $\varepsilon = \varepsilon_b = \varepsilon_c$ ). The transverse momentum of jets  $50\text{GeV} \leq P_{T,j} \leq 60\text{GeV}$ . The test cone size  $r = 0.3$ . The jets from background to  $e^+e^- \rightarrow Zh \rightarrow Zjj$  are not included yet in order to demonstrate the physics more clearly.

It can be found that in Eq.(3) a conservative choice of tagging efficiency ( $\varepsilon = \varepsilon_b = \varepsilon_c \approx 70\%$ ) can decrease the contribution of bottom-jet and charm-jet to the same size as that of gluon-jet, so the extraction of  $\kappa_g$  could become more efficient. However, as shown in Fig.1, while the tagging efficiency become better than 70% the sensitivity of JEP to the Higgs-gluon coupling  $\kappa_g$  will start getting worse. And when the tagging is ideally perfect ( $\varepsilon = 100\%$ ) the JEP becomes independent of  $\kappa_g$ , which is inconvenient for the extraction of  $\kappa_g$  from JEP. This behavior can be understood in Eq.(3) where the b&c-tagging would suppress the contribution from bottom-jet and charm-jet so that the  $\kappa_g$  in the denominator is revealed to just cancel with the one in numerator. One of the direct solutions is to use accumulated JEP, which does not contain  $\kappa_g$  in the denominator. Therefore, we

define the new observable based on accumulated JEP as

$$\Lambda^N(r) \equiv \frac{\sum_j \psi_j(r)}{\sum_j^{\text{SM}} \psi_j(r)}. \quad (5)$$

For the di-jet decay channel of Higgs boson including the b&c-tagging, it can be explicitly expressed as

$$\Lambda^N(r) = \frac{\kappa_g^2 \mathcal{B}_{gg}^{\text{SM}} \psi_g + \mathcal{B}_{q\bar{q}}^{\text{SM}} \psi_q}{\mathcal{B}_{gg}^{\text{SM}} \psi_g + \mathcal{B}_{q\bar{q}}^{\text{SM}} \psi_q}. \quad (6)$$

Now it can be seen that in the ideal condition the perfect tagging can directly simplify this observable  $\Lambda^N(r) = \kappa_g^2$ . In Fig.2 we plot the slope of  $\Lambda^N(r)$  as the sensitivity to  $\kappa_g$  as function of tagging efficiency for the test cone size  $r = 0.3$ . This figure shows that the sensitivity of observable  $\Lambda^N(r)$  to  $\kappa_g$  keeps increasing as the tagging becomes better in the whole region as expected.

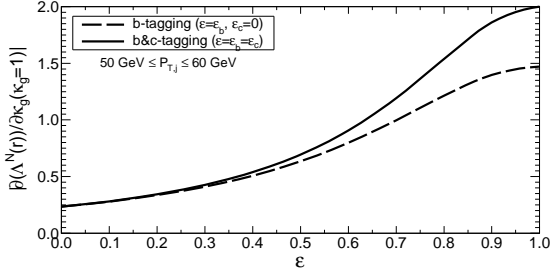


FIG. 2: The slope of  $\Lambda^N(r)$  at  $\kappa_g = 1$  to the efficiency after b-tagging ( $\varepsilon = \varepsilon_b, \varepsilon_c = 0$ ) and b&c-tagging ( $\varepsilon = \varepsilon_b = \varepsilon_c$ ). The transverse momentum of jets  $50\text{GeV} \leq P_{T,j} \leq 60\text{GeV}$ . The test cone size  $r = 0.3$ .

Although the above analysis has shown a promising measurement on  $\kappa_g$  after including b&c-tagging, the background contamination has not been included yet and the light-quark-jet cannot be easily vetoed by b&c-tagging. Therefore, after including the background to Higgs production the Eq.(6) can be extended into

$$\Lambda^N(r) = \frac{\kappa_g^2 \sigma_h \mathcal{B}_{gg}^{\text{SM}} \psi_g + \sigma_h \mathcal{B}_{q\bar{q}}^{\text{SM}} \psi_q + \sigma_{jj}^{\text{BG}} \psi_j^{\text{BG}}}{\sigma_h \mathcal{B}_{gg}^{\text{SM}} \psi_g + \sigma_h \mathcal{B}_{q\bar{q}}^{\text{SM}} \psi_q + \sigma_{jj}^{\text{BG}} \psi_j^{\text{BG}}}, \quad (7)$$

where  $\sigma_h$  is the Higgs production rate at the Higgs factory.  $\sigma_{jj}^{\text{BG}}$  is the production rate of background events [29].  $\psi_j^{\text{BG}}$  includes the jets from background. Although the jets from background explicitly reduce the sensitivity to  $\kappa_g$  in Eq.(7), we found the JEP in each term plays the role of weight for each contribution to  $\Lambda^N$ . Therefore these JEP weights can be shifted to increase the sensitivity to  $\kappa_g$ . For instance, if the JEP is subtracted simultaneously by the average JEP of quark-jets from Higgs decay and jets from background, i.e.  $\tilde{\psi} = (\sigma_h \mathcal{B}_{q\bar{q}}^{\text{SM}} \psi_q + \sigma_{jj}^{\text{BG}} \psi_j^{\text{BG}}) / (\sigma_h \mathcal{B}_{q\bar{q}}^{\text{SM}} + \sigma_{jj}^{\text{BG}})$ , ideally one can obtain the most sensitive measurement on  $\kappa_g$ . However, in practice this subtraction could not be perfect

and the uncertainty of  $\kappa_g$  may not be optimized. Therefore by simultaneously shifting JEP we define a generic observable

$$Z^N(r) = \frac{\sum_j (\psi_j + a)}{\sum_j^{\text{SM}} (\psi_j + a)}, \quad (8)$$

where  $a$  is a tunable parameter.

After including the background contribution, it will be necessary to understand the uncertainty of  $\kappa_g$  extracted from the new observables. As intermediate quantity, the uncertainties of the new observables include the statistical and systematic uncertainties. The evaluation of systematic uncertainties require a detailed detector study and is unknown yet for the Higgs factory. However, the statistical uncertainties can be obtained from MC simulation. Explicitly the new observable  $Z^N(r)$  can be written as

$$Z^N(r) = [N_g(\psi_g + a) + N_q(\psi_q + a) + N_{\text{BG}}(\psi_{\text{BG}} + a)] / C^{\text{SM}}, \quad (9)$$

where the normalization factor

$$C^{\text{SM}} = N_g^{\text{SM}}(\psi_g + a) + N_q^{\text{SM}}(\psi_q + a) + N_{\text{BG}}^{\text{SM}}(\psi_{\text{BG}} + a). \quad (10)$$

$N_g$ ,  $N_q$ , and  $N_{\text{BG}}$  are respectively the number of gluon-jets from Higgs boson decay, quark-jets from Higgs boson decay and jets from background. The total number of jets  $N = N_g + N_q + N_{\text{BG}}$ .

Then the uncertainty of  $Z^N(r)$  is

$$\delta Z^N(r) = \left[ N\sigma^2(r) + N_g(\psi_g + a)^2 + N_q(\psi_q + a)^2 + N_{\text{BG}}(\psi_{\text{BG}} + a)^2 \right]^{1/2} / C^{\text{SM}}. \quad (11)$$

The first term is fluctuation of JEP, which is  $N\sigma^2(r) = N_g^2(\delta\psi_g)^2 + N_q^2(\delta\psi_q)^2 + N_{\text{BG}}^2(\delta\psi_{\text{BG}})^2$ . And the other three terms are fluctuations of relevant event numbers.

Meanwhile the uncertainty on measurement of  $Z^N$  will be passed to the uncertainty on  $\kappa_g$  via the following formula

$$\delta\kappa_g^Z = \delta Z^N \left| \frac{\partial Z^N}{\partial \kappa_g} \right|^{-1}, \quad (12)$$

where the superscript  $Z$  indicates that this uncertainty is obtained by measuring observable  $Z^N$ .

Then the uncertainty of  $\kappa_g$  around the SM prediction  $\kappa_g = 1$  can be explicitly expressed as

$$\delta\kappa_g^Z = \delta\kappa_g^N \left[ \left( \frac{\sigma(r)}{\psi_g + a} \right)^2 + f_g + f_q \left( \frac{\psi_q + a}{\psi_g + a} \right)^2 + f_{\text{BG}} \left( \frac{\psi_{\text{BG}} + a}{\psi_g + a} \right)^2 \right]^{1/2}. \quad (13)$$

where the factor  $\delta\kappa_g^N = \sqrt{N}/2N_g$  is the statistical uncertainty of  $\kappa_g$  via conventional approach and the  $f_g, f_q,$

$f_{\text{BG}}$  are respectively the fraction of gluon-jets from Higgs boson decay, quark-jets from Higgs boson decay and jets from background with respect the total number of jets. When  $r = R$ , JEP will become unity,  $\psi_g = \psi_q = 1$  and  $\sigma(r) = 0$ , the observable  $Z^N$  will be converted to conventional approach.

By tuning the parameter  $a$  we can give a heavier weight to signal and make the size of first term controllable. The minimal uncertainty  $\delta\kappa_g^Z$  can be met at

$$\frac{\partial\delta\kappa_g^Z}{\partial a} = 0, \quad (14)$$

which can provide the solution

$$a = \frac{\sigma^2(r) + f_{\text{BG}}(\psi_q - \psi_{\text{BG}})(\psi_g - \psi_{\text{BG}})}{f_q(\psi_g - \psi_q) + f_{\text{BG}}(\psi_g - \psi_{\text{BG}})} - \psi_q. \quad (15)$$

If the background only contribute quark-jets, this solution can be simplified as

$$a = \frac{\sigma^2(r)}{(\psi_g - \psi_q)f_{\text{B}}} - \psi_q, \quad (16)$$

where

$$f_{\text{B}} = (N_b + N_c + N_{\text{BG}})/N. \quad (17)$$

Then

$$\delta\kappa_g^Z = \delta\kappa_g^N \left\{ 1 - f_{\text{B}} \left[ 1 + \frac{\sigma^2(r)}{(\psi_g - \psi_q)^2 f_{\text{B}}} \right]^{-1} \right\}^{1/2}. \quad (18)$$

If the background is much bigger than signal, the fraction  $f_{\text{B}}$  is approximately equal to 1. The uncertainty of  $\kappa_g$  can be simplified as

$$\delta\kappa_g^Z \approx \delta\kappa_g^N \left[ 1 + \frac{(\psi_g - \psi_q)^2}{\sigma^2(r)} \right]^{-1/2}. \quad (19)$$

It shows that the new observable  $Z^N(r)$  will get a much improvement than the conventional approach if the difference of JEP between quark and gluon is big and the uncertainty of JEP is small. Suppose  $\sigma(r) \ll |\psi_g - \psi_q|$ , the expansion of  $\delta\kappa_g^Z$  is

$$\delta\kappa_g^Z = \delta\kappa_g^N \left[ \frac{\sigma(r)}{|\psi_g - \psi_q|} + \mathcal{O} \right]. \quad (20)$$

The Eq.(20) that ignores the higher-order terms is equivalent to setting the parameter  $a = -\psi_q$  in Eq.(13). Then the  $Z^N(a = -\psi_q)$  will be a perfect observable to reduce the uncertainty of  $\kappa_g$  in this case. However, if  $\sigma(r)$  and  $|\psi_g - \psi_q|$  are at the same order so that the higher-order terms of Eq.(20) can not be ignored, the  $Z^N(a = -\psi_q)$  will transfer a quite large uncertainty to  $\kappa_g$ .

For other specific values of  $a$ , the observable  $Z^N$  will degrade to some simple observables, for example,  $\Lambda^N =$

$Z^N(a = 0)$ . The uncertainty of  $\kappa_g$  via measuring observable  $\Lambda^N$  can be explicitly shown as

$$\delta\kappa_g^\Lambda = \delta\kappa_g^N \left[ \left( \frac{\sigma(r)}{\psi_g} \right)^2 + f_g + f_q \left( \frac{\psi_q}{\psi_g} \right)^2 + f_{\text{BG}} \left( \frac{\psi_{\text{BG}}}{\psi_g} \right)^2 \right]^{1/2}. \quad (21)$$

Since the quark-jet is usually narrower than the gluon-jet, i.e.  $\psi_q > \psi_g$ , the ratios  $\psi_q/\psi_g$  and  $\psi_{\text{BG}}/\psi_g$  will give heavier weights to quark-jets from Higgs boson decay and background-jets. Therefore this observable  $\Lambda^N$  will be a little worse than conventional approach.

In order to give heavier weights to gluon-jets, another interesting observable is choosing the part of jet that lies outside the test cone of size  $r$ , which equals  $Y^N = Z^N(a = -1)$ .

$$Y^N(r) = \frac{\sum_j (1 - \psi_j)}{\sum_j^{\text{SM}} (1 - \psi_j)}. \quad (22)$$

Similarly the uncertainty of  $\kappa_g$  via measuring observable  $Y^N$  can be explicitly shown as

$$\delta\kappa_g^Y = \delta\kappa_g^N \left[ \left( \frac{\sigma(r)}{1 - \psi_g} \right)^2 + f_g + f_q \left( \frac{1 - \psi_q}{1 - \psi_g} \right)^2 + f_{\text{BG}} \left( \frac{1 - \psi_{\text{BG}}}{1 - \psi_g} \right)^2 \right]^{1/2}. \quad (23)$$

In this observable the signal will obtain a heavier weight than the background. Therefore the observable  $Y^N$  is expected to be more sensitive to  $\kappa_g$  than observable  $\Lambda^N$ .

## SIMULATION

In this section we will investigate the new observables based on accumulated JEP proposed in previous section by analyzing Standard Model MC events, which are generated by Whizard 1.95 and showered by Pythia 6 at the future  $e^+e^-$  colliders [11–19] for the center-of-mass energy 250 GeV and integrated luminosity 5  $\text{ab}^{-1}$ . The signal events are classified into three channels according to  $Z$  boson decays:  $Z \rightarrow e^+e^-$  and  $Z \rightarrow \mu^+\mu^-$ . The background events to  $Zh$  production are described in Ref.[13].

The event reconstruction procedure first selects the isolated leptons with energy more than 10 GeV. The two opposite charged ones of the isolated leptons are selected to reconstruct the  $Z$  boson by minimizing[30]

$$\chi^2(M_{\ell^+\ell^-}) = \frac{(M_{\ell^+\ell^-} - M_Z)^2}{\sigma_{M_{\ell^+\ell^-}}^2} + \frac{(M_{\text{h,rec}} - M_h)^2}{\sigma_{M_{\text{h,rec}}}^2}, \quad (24)$$

where  $\sigma_{M_{\ell^+\ell^-}}$  and  $\sigma_{M_{\text{h,rec}}}$  are the Gaussian fits to the distribution of  $M_{\ell^+\ell^-}$  and  $M_{\text{h,rec}}$ . Here  $M_{\text{h,rec}}$  is the recoil mass for the hypothetical Higgs boson via the kinematic relation. After finding the lepton pair, the rest

of final states are clustered into jets by using anti-kt algorithm[31] with cone size  $R = 1.5$  and the energy of every jet is required more than 5 GeV. Clustering jets with a big cone size since it is helpful to reconstruct Higgs boson at lepton colliders. Two jets, whose invariant mass is close to the Higgs mass and recoil mass is close to Z boson mass at the same time, will be selected. Then the following kinematic cuts are applied to reject the backgrounds.

- The lepton pair invariant mass  $M_{\ell^+\ell^-} \in [73,120]$  GeV.
- The transverse momentum of lepton pair  $P_T^{\ell^+\ell^-} \in [10, 70]$  GeV.
- The value of gradient boosted decision trees (BDTG)  $\in [-0.25,1]$ .
- The lepton pair recoil mass  $M_{h,\text{rec}} \in [110,155]$  GeV.
- The total energy of all the visible particles except the lepton pair  $E_{\text{vis}} > 10$  GeV.
- The polar angle of leading and subleading selected jets  $\cos\theta \in [-0.98, 0.98]$ .
- The energy of leading selected jet  $E_j \geq 45$  GeV.
- The energy of subleading selected jet  $E_{\text{sub},j} \geq 15$  GeV.
- The two jets invariant mass  $M_{jj} \in [95, 130]$  GeV.
- The two jets recoil mass  $M_{jj} \in [85, 130]$  GeV.

The mistag efficiency of charm quark to bottom quark is  $\varepsilon_{c \rightarrow b} = 10\%$  and light quark to bottom quark is  $\varepsilon_{q \rightarrow b} = 0$  when b-tagging efficiency is  $\varepsilon_b = 80\%$ . And the mistag efficiency of bottom quark to charm quark is  $\varepsilon_{b \rightarrow c} = 12\%$  and light quark to charm quark is  $\varepsilon_{q \rightarrow c} = 7\%$  when c-tagging efficiency is  $\varepsilon_c = 60\%$ .

The JEP approach contains two aspects: JEP cut and JEP weight. The JEP cut is adding a unique cut which requires the JEP of leading and subleading jets  $\psi_j \in [0.05, 0.99]$  in every event. This cut can effectively remove the background-jets by analyzing the internal structure of jets and decrease the JEP uncertainty  $\sigma(r)$ . The JEP weight means quark-jets and gluon-jets are given different weights by the new observables. And the parameter  $a$  can be tuned to give a heavier weight to gluon-jets as we have already analyzed at previous section.

Fig.3 shows the ratios of JEP uncertainties  $\sigma(r)$  with respect to the difference of JEP between quark-jets and gluon-jets  $|\psi_g - \psi_q|$  vary with the JEP test cone  $r$ . The ratios in different channels all increase as test cone increases and have similar value at test cone  $0.2 \sim 0.4$ . The ratios in electron channel is higher than that in muon channel at the test cone region  $0.4 \sim 0.9$  and the gap is growing as the test cone increases. The ratios in

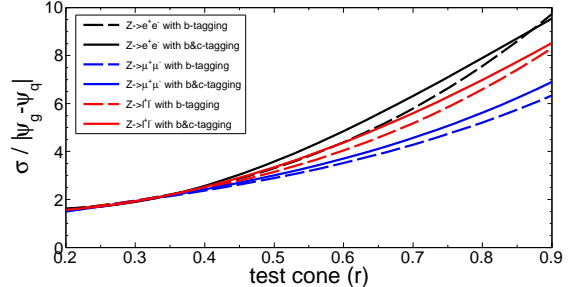


FIG. 3: The ratios of JEP uncertainties with respect to the difference of JEP between quark-jets and gluon-jets after using the JEP cut varies with the JEP test cone  $r$  in different channels of Z boson decay by implementing only b-tagging ( $\varepsilon_b = 80\%$ ) (dotted line) and both b-tagging ( $\varepsilon_b = 80\%$ ) and c-tagging ( $\varepsilon_c = 60\%$ ) (solid line).

$Z \rightarrow \ell^+\ell^-$  channel, which combines the two lepton channels  $Z \rightarrow e^+e^-$  and  $Z \rightarrow \mu^+\mu^-$ , are between that in electron and muon channels. For the same channel, implementing both b-tagging and c-tagging (solid line) will have a higher ratio than only implementing b-tagging. To make sure that the ratios are as small as possible and more events survive after the JEP cut, the test cone is chosen as  $r=0.3$  for the following analysis.

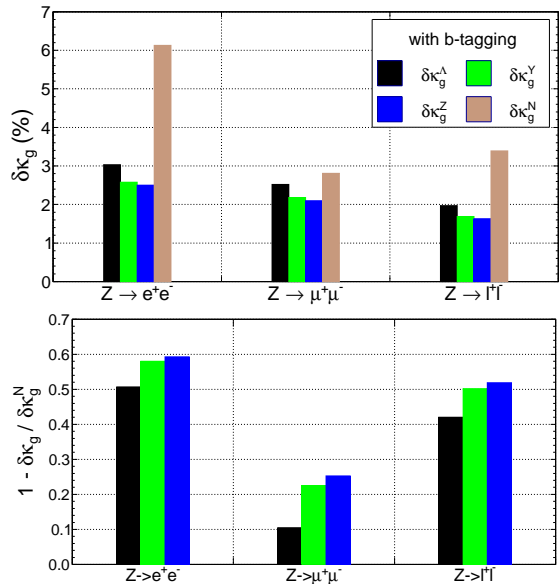


FIG. 4: The uncertainties of Higgs-gluon effective coupling via different observables (above) and their improvements with respect to  $\delta\kappa_g^N$  (below) at test cone  $r = 0.3$  in different channels of Z boson decay by implementing only b-tagging ( $\varepsilon_b = 80\%$ ).

Fig.4 shows the uncertainties of  $\kappa_g$  measurement via different observables (above) and their improvements with respect to  $\delta\kappa_g^N$  (below) at test cone  $r = 0.3$  in different Z boson decay channels by implementing only b-tagging. The uncertainties of  $\kappa_g$  via conventional approach in electron, muon and lepton channel are respec-

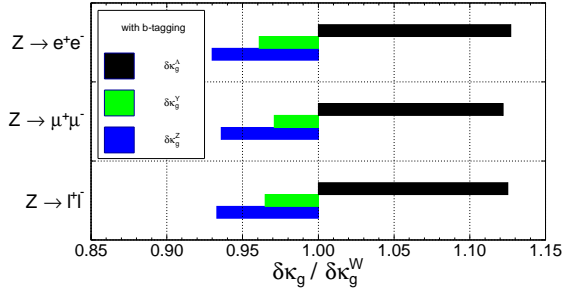


FIG. 5: The ratios of Higgs-gluon effective coupling uncertainties via different observables with respect to  $\delta\kappa_g^W$  at test cone  $r = 0.3$  in different channels of  $Z$  boson decay by implementing only b-tagging ( $\varepsilon_b = 80\%$ ).

tively 6.1%, 2.8% and 3.4%. The uncertainties in the electron channel are much bigger than those in the muon channel since the bhabha background (final state is  $e^+$ ,  $e^-$  and their radiations) has a very large cross section and a sizable number of events still survive after all the kinematic cuts. However, the JEP cut can effectively remove this kind of background by analyzing the internal structure of jets, since most of these background-jets are constituted by only one or a few particles (photon) near the jet axis and given the JEP values very close to both ends. Therefore, all the new observables will provide remarkable improvements on the conventional approach. Especially electron channel, new observables  $\Lambda^N$ ,  $Y^N$  and  $Z^N$  are respectively get 51%, 58% and 59% improvements than conventional approach. When we combine the lepton channels, the uncertainty of  $\kappa_g$  can be measured to 1.6% via the optimized observable  $Z^N$ .

The improvement of JEP approach comes from JEP cut and JEP weight. To separate contributions of the two factors,  $\delta\kappa_g^W = \sqrt{N^{\text{JEP-cut}}/2N_g^{\text{JEP-cut}}}$  is used to express the uncertainty of  $\kappa_g$  only with JEP cut.  $N_g^{\text{JEP-cut}}$  and  $N^{\text{JEP-cut}}$  are respectively the number of gluon-jets from Higgs boson decay and total number of jets after the JEP cut. In Fig.5, it can be seen that observable  $\Lambda^N$  gets a bigger uncertainties of  $\kappa_g$  than  $\delta\kappa_g^W$  by about 12% for the total lepton channel. As we have already analyzed at last section, due to  $\psi_q > \psi_g$ , the ratios  $\psi_q/\psi_g$  and  $\psi_{\text{BG}}/\psi_g$  give heavier weights to quark-jets from Higgs boson decay and background-jets. And since  $\psi_q$  and  $\psi_{\text{BG}}$  are bigger than  $\psi_g$  by about 13%, the observable  $\Lambda^N$  gets a little bigger uncertainties of  $\kappa_g$  than other new observables. The ratios  $(1 - \psi_q)/(1 - \psi_g)$  and  $(1 - \psi_{\text{BG}})/(1 - \psi_g)$  in observable  $Y^N$  give lighter weights to quark-jets from Higgs boson decay and background-jets, so the  $\kappa_g$  uncertainties using observable  $Y^N$  have about 4% improvement than  $\delta\kappa_g^W$  for the total lepton channel. After tuning the parameter  $a$ , the observable  $Z^N$  is indeed the most optimized one compared to the other observables and the  $\kappa_g$  uncertainties using observable  $Z^N$  have about 7% improvement than  $\delta\kappa_g^W$  for the

total lepton channel. Therefore this optimized observable  $Z^N$  is a very promising approach to assist the  $\kappa_g$  measurement.

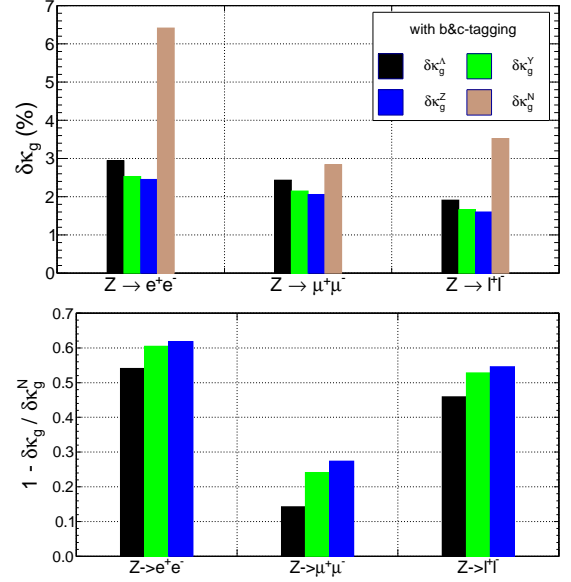


FIG. 6: The uncertainties of Higgs-gluon effective coupling via different observables (above) and their improvements with respect to  $\delta\kappa_g^N$  (below) at test cone  $r = 0.3$  in different channels of  $Z$  boson decay by implementing both b-tagging ( $\varepsilon_b = 80\%$ ) and c-tagging ( $\varepsilon_c = 60\%$ ).

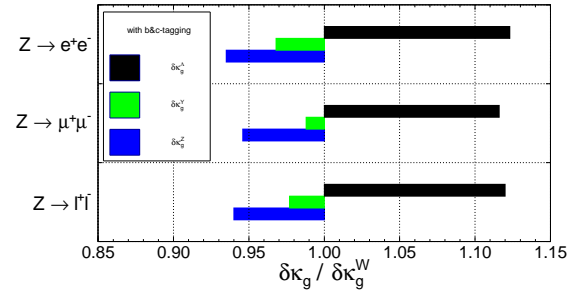


FIG. 7: The ratios of Higgs-gluon effective coupling uncertainties via different observables with respect to  $\delta\kappa_g^W$  at test cone  $r = 0.3$  in different channels of  $Z$  boson decay by implementing both b-tagging ( $\varepsilon_b = 80\%$ ) and c-tagging ( $\varepsilon_c = 60\%$ ).

Fig.6 presents  $\kappa_g$  uncertainties via different observables (above) and their improvements with respect to conventional approach  $\delta\kappa_g^N$  (below) including the b&c-tagging. Compared with Fig.4, it can be seen that the uncertainties of  $\kappa_g$  via conventional approach increase by about 5% after c-tagging, although the c-tagging can efficiently reduce the contamination of charm-jets and the background-jets. This is because the c-tagging does not only veto the charm-jets, but it also excludes some of the gluon-jets since its mistag rate for light-quark-jet and gluon-jet is 7%. But the opposite is the uncertainties of  $\kappa_g$  via new observables decrease by about 2% after c-

tagging. From the comparison between Fig.5 and Fig.7, we find that the contributions of JEP weight decrease by about 10% after c-tagging. This means that c-tagging can increase contributions of JEP cut but decrease the contributions of JEP weight, which leads to the effect from c-tagging is not obvious. In the future if the mistag rate of c-tagging can be improved enough, the c-tagging may further help the  $\kappa_g$  measurement.

## CONCLUSIONS

In this paper, we propose to use accumulated JEP for the measurement of the Higgs-gluon effective coupling. By using the optimized observable  $Z^N$  in the MC simulation at the future  $e^+e^-$  colliders for the center-of-mass energy 250 GeV and integrated luminosity  $5 \text{ ab}^{-1}$ , the statistical uncertainties of effective coupling  $\kappa_g$  can reach about 1.6% in the channels of  $Z$  boson decaying to lepton pairs and is totally reduced by about 52% (45% from the JEP cut contribution and 7% from the JEP weight contribution) compared to the relevant  $\kappa_g$  uncertainties in conventional approach. In this work, our MC simulation has not yet included the template fit, which can further reduce the  $\kappa_g$  uncertainties by about 68%. If naively implementing this improvement ratio, the  $\kappa_g$  uncertainties via the optimized observable  $Z^N$  can be expected to reach 1.1% after using template fit. And this will be investigated in detail in our future work.

*Acknowledgments:* This work was supported by the National Natural Science Foundation of China under Grant No. 11675185. Y.W. is supported by the China Postdoctoral Science Foundation under Grant No. 2016M601134, and an International Postdoctoral Exchange Fellowship Program between the Office of the National Administrative Committee of Postdoctoral Researchers of China (ONACPR) and DESY. X.Z. has received funding from the European Union's Horizon 2020 research and innovation programme as part of the Marie Skłodowska-Curie Innovative Training Network MCnetITN3 (grant agreement no. 722104). The authors want to thank Gang Li and Manqi Ruan for helpful discussions and the complete MC simulation events.

---

\* Electronic address: ligx@ihep.ac.cn

† Electronic address: zhaoli@ihep.ac.cn

‡ Electronic address: ydliu@bnu.edu.cn

§ Electronic address: wangyan728@ihep.ac.cn

¶ Electronic address: xiaoran.zhao@uclouvain.be

- [1] M. B. Einhorn, in *Conference on Unified Symmetry in the Small and in the Large Coral Gables, Florida, January 25-27, 1993* (1993), pp. 407–420, hep-ph/9303323.  
 [2] S. Kanemura, Y. Okada, E. Senaha, and C. P. Yuan, Phys. Rev. **D70**, 115002 (2004).

- [3] X.-G. He, Y. Tang, and G. Valencia, Phys. Rev. **D88**, 033005 (2013).  
 [4] A. Moyotl, S. Chamorro, H. Castilla-Valdez, and M. A. Prez (2016), 1610.06299.  
 [5] S. Baek and X.-B. Yuan, Phys. Lett. **B774**, 662 (2017).  
 [6] W.-S. Hou and M. Kikuchi, Phys. Rev. **D96**, 015033 (2017).  
 [7] S. Kanemura, M. Kikuchi, K. Sakurai, and K. Yagyu, Phys. Rev. **D96**, 035014 (2017).  
 [8] S. Paehr and G. Weiglein (2017), 1705.07909.  
 [9] M. E. Peskin (2012), 1207.2516.  
 [10] M. E. Peskin, in *Proceedings, 2013 Community Summer Study on the Future of U.S. Particle Physics: Snowmass on the Mississippi (CSS2013): Minneapolis, MN, USA, July 29-August 6, 2013* (2013), 1312.4974.  
 [11] *CEPC-SPPC Preliminary Conceptual Design Report. 1. Physics and Detector* (2015), IHEP-CEPC-DR-2015-01, IHEP-TH-2015-01, IHEP-EP-2015-01.  
 [12] *CEPC-SPPC Preliminary Conceptual Design Report. 2. Accelerator* (2015), IHEP-CEPC-DR-2015-01, IHEP-AC-2015-01.  
 [13] X. Mo, G. Li, M.-Q. Ruan, and X.-C. Lou, Chin. Phys. **C40**, 033001 (2016).  
 [14] M. Bicer et al. (TLEP Design Study Working Group), JHEP **01**, 164 (2014).  
 [15] W. Barletta, M. Battaglia, M. Klute, M. Mangano, S. Prestemon, L. Rossi, and P. Skands, Nucl. Instrum. Meth. **A764**, 352 (2014).  
 [16] M. Benedikt and F. Zimmermann, PoS **LeptonPhoton2015**, 052 (2016).  
 [17] T. Behnke, J. E. Brau, B. Foster, J. Fuster, M. Harrison, J. M. Paterson, M. Peskin, M. Stanitzki, N. Walker, and H. Yamamoto (2013), 1306.6327.  
 [18] C. Adolphsen, M. Barone, B. Barish, K. Buesser, P. Burrows, J. Carwardine, J. Clark, H. Mainaud Durand, G. Dugan, E. Elsen, et al. (2013), 1306.6328.  
 [19] H. Abramowicz et al. (2013), 1306.6329.  
 [20] Y. Bai (CEPC Working Group), *Measurements of the decay branching fraction of  $H \rightarrow b\bar{b}/c\bar{c}/gg$  at CEPC (CEPC Note in preparation)* (2017).  
 [21] G. Aad et al. (ATLAS), Eur. Phys. J. **C76**, 6 (2016).  
 [22] G. Aad et al. (ATLAS, CMS), JHEP **08**, 045 (2016).  
 [23] V. Rentala, N. Vignaroli, H.-n. Li, Z. Li, and C. P. Yuan, Phys. Rev. **D88**, 073007 (2013).  
 [24] P. Agrawal and V. Rentala, JHEP **05**, 098 (2014).  
 [25] R. S. Chivukula, E. H. Simmons, and N. Vignaroli, in *Sakata Memorial KMI Workshop on Origin of Mass and Strong Coupling Gauge Theories (SCGT15) Nagoya, Japan, March 3-6, 2015* (2015), 1507.06522.  
 [26] V. Khachatryan et al. (CMS), Eur. Phys. J. **C75**, 212 (2015).  
 [27] T. A. collaboration (ATLAS) (2015).  
 [28] H.-n. Li, Z. Li, and C. P. Yuan, Phys. Rev. Lett. **107**, 152001 (2011).  
 [29] G. L. Xin Mo (CEPC Working Group), *Generated Sample Stauts for CEPC Simulation Studies (CEPC Note in preparation)* (2017).  
 [30] J. Yan, S. Watanuki, K. Fujii, A. Ishikawa, D. Jeans, J. Strube, J. Tian, and H. Yamamoto, Phys. Rev. **D94**, 113002 (2016).  
 [31] M. Cacciari, G. P. Salam, and G. Soyez, Eur. Phys. J. **C72**, 1896 (2012).